

Study of $e^+e^- \rightarrow \pi^0 X(3872)\gamma$ and search for $Z_c(4020)^0 \rightarrow X(3872)\gamma$

M. Ablikim,¹ M. N. Achasov,^{10,c} P. Adlarson,⁶⁷ S. Ahmed,¹⁵ M. Albrecht,⁴ R. Aliberti,²⁸ A. Amoroso,^{66a,66c} M. R. An,³² Q. An,^{63,49} X. H. Bai,⁵⁷ Y. Bai,⁴⁸ O. Bakina,²⁹ R. Baldini Ferroli,^{23a} I. Balossino,^{24a} Y. Ban,^{38,k} K. Begzsuren,²⁶ N. Berger,²⁸ M. Bertani,^{23a} D. Bettoni,^{24a} F. Bianchi,^{66a,66c} J. Biernat,⁶⁷ J. Bloms,⁶⁰ A. Bortone,^{66a,66c} I. Boyko,²⁹ R. A. Briere,⁵ H. Cai,⁶⁸ X. Cai,^{1,49} A. Calcaterra,^{23a} G. F. Cao,^{1,54} N. Cao,^{1,54} S. A. Cetin,^{53a} J. F. Chang,^{1,49} W. L. Chang,^{1,54} G. Chelkov,^{29,b} D. Y. Chen,⁶ G. Chen,¹ H. S. Chen,^{1,54} M. L. Chen,^{1,49} S. J. Chen,³⁵ X. R. Chen,²⁵ Y. B. Chen,^{1,49} Z. J. Chen,^{20,1} W. S. Cheng,^{66c} G. Cibinetto,^{24a} F. Cossio,^{66c} X. F. Cui,³⁶ H. L. Dai,^{1,49} X. C. Dai,^{1,54} A. Dbeysy,¹⁵ R. E. de Boer,⁴ D. Dedovich,²⁹ Z. Y. Deng,¹ A. Denig,²⁸ I. Denysenko,²⁹ M. Destefanis,^{66a,66c} F. De Mori,^{66a,66c} Y. Ding,³³ C. Dong,³⁶ J. Dong,^{1,49} L. Y. Dong,^{1,54} M. Y. Dong,^{1,49,54} X. Dong,⁶⁸ S. X. Du,⁷¹ Y. L. Fan,⁶⁸ J. Fang,^{1,49} S. S. Fang,^{1,54} Y. Fang,¹ R. Farinelli,^{24A} L. Fava,^{66b,66c} F. Feldbauer,⁴ G. Felici,^{23a} C. Q. Feng,^{63,49} J. H. Feng,⁵⁰ M. Fritsch,⁴ C. D. Fu,¹ Y. Gao,^{38,k} Y. Gao,^{63,49} Y. Gao,⁶⁴ Y. G. Gao,⁶ I. Garzia,^{24a,24b} P. T. Ge,⁶⁸ C. Geng,⁵⁰ E. M. Gersabeck,⁵⁸ A. Gilman,⁵⁹ K. Goetzen,¹¹ L. Gong,³³ W. X. Gong,^{1,49} W. Gradl,²⁸ M. Greco,^{66a,66c} L. M. Gu,³⁵ M. H. Gu,^{1,49} S. Gu,² Y. T. Gu,¹³ C. Y. Guan,^{1,54} A. Q. Guo,²² L. B. Guo,³⁴ R. P. Guo,⁴⁰ Y. P. Guo,^{9,h} A. Guskov,^{29,b} T. T. Han,⁴¹ W. Y. Han,³² X. Q. Hao,¹⁶ F. A. Harris,⁵⁶ N. Hüsken,⁶⁰ K. L. He,^{1,54} F. H. Heinsius,⁴ C. H. Heinz,²⁸ T. Held,⁴ Y. K. Heng,^{1,49,54} C. Herold,⁵¹ M. Himmelreich,^{11,f} T. Holtmann,⁴ G. Y. Hou,^{1,54} Y. R. Hou,⁵⁴ Z. L. Hou,¹ H. M. Hu,^{1,54} J. F. Hu,^{47,m} T. Hu,^{1,49,54} Y. Hu,¹ G. S. Huang,^{63,49} L. Q. Huang,⁶⁴ X. T. Huang,⁴¹ Y. P. Huang,¹ Z. Huang,^{38,k} T. Hussain,⁶⁵ W. Ikegami Andersson,⁶⁷ W. Imoehl,²² M. Irshad,^{63,49} S. Jaeger,⁴ S. Janchiv,^{26,j} Q. Ji,¹ Q. P. Ji,¹⁶ X. B. Ji,^{1,54} X. L. Ji,^{1,49} Y. Y. Ji,⁴¹ H. B. Jiang,⁴¹ X. S. Jiang,^{1,49,54} J. B. Jiao,⁴¹ Z. Jiao,¹⁸ S. Jin,³⁵ Y. Jin,⁵⁷ M. Q. Jing,^{1,54} T. Johansson,⁶⁷ N. Kalantar-Nayestanaki,⁵⁵ X. S. Kang,³³ R. Kappert,⁵⁵ M. Kavatsyuk,⁵⁵ B. C. Ke,^{43,1} I. K. Keshk,⁴ A. Khoukaz,⁶⁰ P. Kiese,²⁸ R. Kiuchi,¹ R. Kliemt,¹¹ L. Koch,³⁰ O. B. Kolcu,^{53a,e} B. Kopf,⁴ M. Kuemmel,⁴ M. Kuessner,⁴ A. Kupsc,⁶⁷ M. G. Kurth,^{1,54} W. Kühn,³⁰ J. J. Lane,⁵⁸ J. S. Lange,³⁰ P. Larin,¹⁵ A. Lavanaia,²¹ L. Lavezzi,^{66a,66c} Z. H. Lei,^{63,49} H. Leithoff,²⁸ M. Lellmann,²⁸ T. Lenz,²⁸ C. Li,³⁹ C. H. Li,³² Cheng Li,^{63,49} D. M. Li,⁷¹ F. Li,^{1,49} G. Li,¹ H. Li,^{63,49} H. Li,⁴³ H. B. Li,^{1,54} H. J. Li,^{9,h} J. L. Li,⁴¹ J. Q. Li,⁴ J. S. Li,⁵⁰ Ke Li,¹ L. K. Li,¹ Lei Li,³ P. R. Li,³¹ S. Y. Li,⁵² W. D. Li,^{1,54} W. G. Li,¹ X. H. Li,^{63,49} X. L. Li,⁴¹ Xiaoyu Li,^{1,54} Z. Y. Li,⁵⁰ H. Liang,^{1,54} H. Liang,^{63,49} H. Liang,²⁷ Y. F. Liang,⁴⁵ Y. T. Liang,²⁵ G. R. Liao,¹² L. Z. Liao,^{1,54} J. Libby,²¹ C. X. Lin,⁵⁰ B. J. Liu,¹ C. X. Liu,¹ D. Liu,^{63,49} F. H. Liu,⁴⁴ Fang Liu,¹ Feng Liu,⁶ H. B. Liu,¹³ H. M. Liu,^{1,54} Huanhuan Liu,¹ Huihui Liu,¹⁷ J. B. Liu,^{63,49} J. L. Liu,⁶⁴ J. Y. Liu,^{1,54} K. Liu,¹ K. Y. Liu,³³ L. Liu,^{63,49} M. H. Liu,^{9,h} P. L. Liu,¹ Q. Liu,⁵⁴ Q. Liu,⁶⁸ S. B. Liu,^{63,49} Shuai Liu,⁴⁶ T. Liu,^{1,54} W. M. Liu,^{63,49} X. Liu,³¹ Y. Liu,³¹ Y. B. Liu,³⁶ Z. A. Liu,^{1,49,54} Z. Q. Liu,⁴¹ X. C. Lou,^{1,49,54} F. X. Lu,¹⁶ F. X. Lu,⁵⁰ H. J. Lu,¹⁸ J. D. Lu,^{1,54} J. G. Lu,^{1,49} X. L. Lu,¹ Y. Lu,¹ Y. P. Lu,^{1,49} C. L. Luo,³⁴ M. X. Luo,⁷⁰ P. W. Luo,⁵⁰ T. Luo,^{9,h} X. L. Luo,^{1,49} S. Lusso,^{66c} X. R. Lyu,⁵⁴ F. C. Ma,³³ H. L. Ma,¹ L. L. Ma,⁴¹ M. M. Ma,^{1,54} Q. M. Ma,¹ R. Q. Ma,^{1,54} R. T. Ma,⁵⁴ X. X. Ma,^{1,54} X. Y. Ma,^{1,49} F. E. Maas,¹⁵ M. Maggiora,^{66a,66c} S. Maldaner,⁴ S. Malde,⁶¹ Q. A. Malik,⁶⁵ A. Mangoni,^{23b} Y. J. Mao,^{38,k} Z. P. Mao,¹ S. Marcello,^{66a,66c} Z. X. Meng,⁵⁷ J. G. Messchendorp,⁵⁵ G. Mezzadri,^{24a} T. J. Min,³⁵ R. E. Mitchell,²² X. H. Mo,^{1,49,54} Y. J. Mo,⁶ N. Yu. Muchnoi,^{10,c} H. Muramatsu,⁵⁹ S. Nakhoul,^{11,f} Y. Nefedov,²⁹ F. Nerling,^{11,f} I. B. Nikolaev,^{10,c} Z. Ning,^{1,49} S. Nisar,^{8,1} S. L. Olsen,⁵⁴ Q. Ouyang,^{1,49,54} S. Pacetti,^{23b,23c} X. Pan,^{9,h} Y. Pan,⁵⁸ A. Pathak,¹ P. Patteri,^{23a} M. Pelizaeus,⁴ H. P. Peng,^{63,49} K. Peters,^{11,f} J. Pettersson,⁶⁷ J. L. Ping,³⁴ R. G. Ping,^{1,54} R. Poling,⁵⁹ V. Prasad,^{63,49} H. Qi,^{63,49} H. R. Qi,⁵² K. H. Qi,²⁵ M. Qi,³⁵ T. Y. Qi,² T. Y. Qi,⁹ S. Qian,^{1,49} W. B. Qian,⁵⁴ Z. Qian,⁵⁰ C. F. Qiao,⁵⁴ L. Q. Qin,¹² X. P. Qin,⁹ X. S. Qin,⁴¹ Z. H. Qin,^{1,49} J. F. Qiu,¹ S. Q. Qu,³⁶ K. H. Rashid,⁶⁵ K. Ravindran,²¹ C. F. Redmer,²⁸ A. Rivetti,^{66c} V. Rodin,⁵⁵ M. Rolo,^{66c} G. Rong,^{1,54} Ch. Rosner,¹⁵ M. Rump,⁶⁰ H. S. Sang,⁶³ A. Sarantsev,^{29,d} Y. Schelhaas,²⁸ C. Schnier,⁴ K. Schoenning,⁶⁷ M. Scodreggio,^{24a,24b} D. C. Shan,⁴⁶ W. Shan,¹⁹ X. Y. Shan,^{63,49} J. F. Shangguan,⁴⁶ M. Shao,^{63,49} C. P. Shen,⁹ H. F. Shen,^{1,54} P. X. Shen,³⁶ X. Y. Shen,^{1,54} H. C. Shi,^{63,49} R. S. Shi,^{1,54} X. Shi,^{1,49} X. D. Shi,^{63,49} J. J. Song,⁴¹ W. M. Song,^{27,1} Y. X. Song,^{38,k} S. Sosio,^{66a,66c} S. Spataro,^{66a,66c} K. X. Su,⁶⁸ P. P. Su,⁴⁶ F. F. Sui,⁴¹ G. X. Sun,¹ H. K. Sun,¹ J. F. Sun,¹⁶ L. Sun,⁶⁸ S. S. Sun,^{1,54} T. Sun,^{1,54} W. Y. Sun,²⁷ W. Y. Sun,³⁴ X. Sun,^{20,1} Y. J. Sun,^{63,49} Y. K. Sun,^{63,49} Y. Z. Sun,¹ Z. T. Sun,¹ Y. H. Tan,⁶⁸ Y. X. Tan,^{63,49} C. J. Tang,⁴⁵ G. Y. Tang,¹ J. Tang,⁵⁰ J. X. Tang,^{63,49} V. Thoren,⁶⁷ W. H. Tian,⁴³ I. Uman,^{53b} B. Wang,¹ C. W. Wang,³⁵ D. Y. Wang,^{38,k} H. J. Wang,³¹ H. P. Wang,^{1,54} K. Wang,^{1,49} L. L. Wang,¹ M. Wang,⁴¹ M. Z. Wang,^{38,k} Meng Wang,^{1,54} W. Wang,⁵⁰ W. H. Wang,⁶⁸ W. P. Wang,^{63,49} X. Wang,^{38,k} X. F. Wang,³¹ X. L. Wang,^{9,h} Y. Wang,^{63,49} Y. Wang,⁵⁰ Y. D. Wang,³⁷ Y. F. Wang,^{1,49,54} Y. Q. Wang,¹ Y. Y. Wang,³¹ Z. Wang,^{1,49} Z. Y. Wang,¹ Ziyi Wang,⁵⁴ Zongyuan Wang,^{1,54} D. H. Wei,¹² P. Weidenkaff,²⁸ F. Weidner,⁶⁰ S. P. Wen,¹ D. J. White,⁵⁸ U. Wiedner,⁴ G. Wilkinson,⁶¹ M. Wolke,⁶⁷ L. Wollenberg,⁴ J. F. Wu,^{1,54} L. H. Wu,¹ L. J. Wu,^{1,54} X. Wu,^{9,h} Z. Wu,^{1,49} L. Xia,^{63,49} H. Xiao,^{9,h} S. Y. Xiao,¹ Z. J. Xiao,³⁴ X. H. Xie,^{38,k} Y. G. Xie,^{1,49} Y. H. Xie,⁶ T. Y. Xing,^{1,54} G. F. Xu,¹ Q. J. Xu,¹⁴ W. Xu,^{1,54} X. P. Xu,⁴⁶ Y. C. Xu,⁵⁴ F. Yan,^{9,h} L. Yan,^{9,h} W. B. Yan,^{63,49} W. C. Yan,⁷¹ Xu Yan,⁴⁶ H. J. Yang,^{42,g} H. X. Yang,¹ L. Yang,⁴³ S. L. Yang,⁵⁴ Y. X. Yang,¹² Yifan Yang,^{1,54} Zhi Yang,²⁵ M. Ye,^{1,49} M. H. Ye,⁷ J. H. Yin,¹ Z. Y. You,⁵⁰ B. X. Yu,^{1,49,54} C. X. Yu,³⁶ G. Yu,^{1,54} J. S. Yu,^{20,1} T. Yu,⁶⁴ C. Z. Yuan,^{1,54} L. Yuan,² X. Q. Yuan,^{38,k} Y. Yuan,¹ Z. Y. Yuan,⁵⁰ C. X. Yue,³² A. Yuncu,^{53aa} A. A. Zafar,⁶⁵ Zeng,⁶

Y. Zeng,^{20,1} A. Q. Zhang,¹ B. X. Zhang,¹ Guangyi Zhang,¹⁶ H. Zhang,⁶³ H. H. Zhang,⁵⁰ H. H. Zhang,²⁷
 H. Y. Zhang,^{1,49} J. J. Zhang,⁴³ J. L. Zhang,⁶⁹ J. Q. Zhang,³⁴ J. W. Zhang,^{1,49,54} J. Y. Zhang,¹ J. Z. Zhang,^{1,54}
 Jianyu Zhang,^{1,54} Jiawei Zhang,^{1,54} L. Q. Zhang,⁵⁰ Lei Zhang,³⁵ S. Zhang,⁵⁰ S. F. Zhang,³⁵ Shulei Zhang,^{20,1}
 X. D. Zhang,³⁷ X. Y. Zhang,⁴¹ Y. Zhang,⁶¹ Y. H. Zhang,^{1,49} Y. T. Zhang,^{63,49} Yan Zhang,^{63,49} Yao Zhang,¹ Yi Zhang,^{9,h}
 Z. H. Zhang,⁶ Z. Y. Zhang,⁶⁸ G. Zhao,¹ J. Zhao,³² J. Y. Zhao,^{1,54} J. Z. Zhao,^{1,49} Lei Zhao,^{63,49} Ling Zhao,¹
 M. G. Zhao,³⁶ Q. Zhao,¹ S. J. Zhao,⁷¹ Y. B. Zhao,^{1,49} Y. X. Zhao,²⁵ Z. G. Zhao,^{63,49} A. Zhemchugov,^{29,b} B. Zheng,⁶⁴
 J. P. Zheng,^{1,49} Y. Zheng,^{38,k} Y. H. Zheng,⁵⁴ B. Zhong,³⁴ C. Zhong,⁶⁴ L. P. Zhou,^{1,54} Q. Zhou,^{1,54} X. Zhou,⁶⁸ X. K. Zhou,⁵⁴
 X. R. Zhou,^{63,49} A. N. Zhu,^{1,54} J. Zhu,³⁶ K. Zhu,¹ K. J. Zhu,^{1,49,54} S. H. Zhu,⁶² T. J. Zhu,⁶⁹ W. J. Zhu,^{9,h} W. J. Zhu,³⁶
 Y. C. Zhu,^{63,49} Z. A. Zhu,^{1,54} B. S. Zou,¹ and J. H. Zou¹

(BESIII Collaboration)

¹*Institute of High Energy Physics, Beijing 100049, People's Republic of China*

²*Beihang University, Beijing 100191, People's Republic of China*

³*Beijing Institute of Petrochemical Technology, Beijing 102617, People's Republic of China*

⁴*Bochum Ruhr-University, D-44780 Bochum, Germany*

⁵*Carnegie Mellon University, Pittsburgh, Pennsylvania 15213, USA*

⁶*Central China Normal University, Wuhan 430079, People's Republic of China*

⁷*China Center of Advanced Science and Technology, Beijing 100190, People's Republic of China*

⁸*COMSATS University Islamabad, Lahore Campus, Defence Road,
Off Raiwind Road, 54000 Lahore, Pakistan*

⁹*Fudan University, Shanghai 200443, People's Republic of China*

¹⁰*G.I. Budker Institute of Nuclear Physics SB RAS (BINP), Novosibirsk 630090, Russia*

¹¹*GSI Helmholtzcentre for Heavy Ion Research GmbH, D-64291 Darmstadt, Germany*

¹²*Guangxi Normal University, Guilin 541004, People's Republic of China*

¹³*Guangxi University, Nanning 530004, People's Republic of China*

¹⁴*Hangzhou Normal University, Hangzhou 310036, People's Republic of China*

¹⁵*Helmholtz Institute Mainz, Staudinger Weg 18, D-55099 Mainz, Germany*

¹⁶*Henan Normal University, Xixiang 453007, People's Republic of China*

¹⁷*Henan University of Science and Technology, Luoyang 471003, People's Republic of China*

¹⁸*Huangshan College, Huangshan 245000, People's Republic of China*

¹⁹*Hunan Normal University, Changsha 410081, People's Republic of China*

²⁰*Hunan University, Changsha 410082, People's Republic of China*

²¹*Indian Institute of Technology Madras, Chennai 600036, India*

²²*Indiana University, Bloomington, Indiana 47405, USA*

^{23a}*INFN Laboratori Nazionali di Frascati, INFN Laboratori Nazionali di Frascati, I-00044, Frascati, Italy*

^{23b}*INFN Laboratori Nazionali di Frascati, INFN Sezione di Perugia, I-06100, Perugia, Italy*

^{23c}*INFN Laboratori Nazionali di Frascati, University of Perugia, I-06100, Perugia, Italy*

^{24a}*INFN Sezione di Ferrara, INFN Sezione di Ferrara, I-44122, Ferrara*

^{24b}*INFN Sezione di Ferrara, University of Ferrara, I-44122, Ferrara, Italy*

²⁵*Institute of Modern Physics, Lanzhou 730000, People's Republic of China*

²⁶*Institute of Physics and Technology, Peace Ave. 54B, Ulaanbaatar 13330, Mongolia*

²⁷*Jilin University, Changchun 130012, People's Republic of China*

²⁸*Johannes Gutenberg University of Mainz, Johann-Joachim-Becher-Weg 45, D-55099 Mainz, Germany*

²⁹*Joint Institute for Nuclear Research, 141980 Dubna, Moscow region, Russia*

³⁰*Justus-Liebig-Universitaet Giessen, II. Physikalisches Institut,
Heinrich-Buff-Ring 16, D-35392 Giessen, Germany*

³¹*Lanzhou University, Lanzhou 730000, People's Republic of China*

³²*Liaoning Normal University, Dalian 116029, People's Republic of China*

³³*Liaoning University, Shenyang 110036, People's Republic of China*

³⁴*Nanjing Normal University, Nanjing 210023, People's Republic of China*

³⁵*Nanjing University, Nanjing 210093, People's Republic of China*

³⁶*Nankai University, Tianjin 300071, People's Republic of China*

³⁷*North China Electric Power University, Beijing 102206, People's Republic of China*

³⁸*Peking University, Beijing 100871, People's Republic of China*

³⁹*Qufu Normal University, Qufu 273165, People's Republic of China*

⁴⁰*Shandong Normal University, Jinan 250014, People's Republic of China*

⁴¹*Shandong University, Jinan 250100, People's Republic of China*

⁴²*Shanghai Jiao Tong University, Shanghai 200240, People's Republic of China*

- ⁴³*Shanxi Normal University, Linfen 041004, People's Republic of China*
⁴⁴*Shanxi University, Taiyuan 030006, People's Republic of China*
⁴⁵*Sichuan University, Chengdu 610064, People's Republic of China*
⁴⁶*Soochow University, Suzhou 215006, People's Republic of China*
⁴⁷*South China Normal University, Guangzhou 510006, People's Republic of China*
⁴⁸*Southeast University, Nanjing 211100, People's Republic of China*
⁴⁹*State Key Laboratory of Particle Detection and Electronics, Beijing 100049, Hefei 230026, People's Republic of China*
⁵⁰*Sun Yat-Sen University, Guangzhou 510275, People's Republic of China*
⁵¹*Suranaree University of Technology, University Avenue 111, Nakhon Ratchasima 30000, Thailand*
⁵²*Tsinghua University, Beijing 100084, People's Republic of China*
^{53a}*Turkish Accelerator Center Particle Factory Group, Istanbul Bilgi University, 34060 Eyup, Istanbul, Turkey*
^{53b}*Turkish Accelerator Center Particle Factory Group, Near East University, Nicosia, North Cyprus, Mersin 10, Turkey*
⁵⁴*University of Chinese Academy of Sciences, Beijing 100049, People's Republic of China*
⁵⁵*University of Groningen, NL-9747 AA Groningen, Netherlands*
⁵⁶*University of Hawaii, Honolulu, Hawaii 96822, USA*
⁵⁷*University of Jinan, Jinan 250022, People's Republic of China*
⁵⁸*University of Manchester, Oxford Road, Manchester, M13 9PL, United Kingdom*
⁵⁹*University of Minnesota, Minneapolis, Minnesota 55455, USA*
⁶⁰*University of Muenster, Wilhelm-Klemm-Str. 9, 48149 Muenster, Germany*
⁶¹*University of Oxford, Keble Rd, Oxford, United Kingdom OX13RH*
⁶²*University of Science and Technology Liaoning, Anshan 114051, People's Republic of China*
⁶³*University of Science and Technology of China, Hefei 230026, People's Republic of China*
⁶⁴*University of South China, Hengyang 421001, People's Republic of China*
⁶⁵*University of the Punjab, Lahore-54590, Pakistan*
^{66a}*University of Turin and INFN, University of Turin, I-10125, Turin, Italy*
^{66b}*University of Turin and INFN, University of Eastern Piedmont, I-15121, Alessandria, Italy*
^{66c}*University of Turin and INFN, INFN, I-10125, Turin, Italy*
⁶⁷*Uppsala University, Box 516, SE-75120 Uppsala, Sweden*
⁶⁸*Wuhan University, Wuhan 430072, People's Republic of China*
⁶⁹*Xinyang Normal University, Xinyang 464000, People's Republic of China*
⁷⁰*Zhejiang University, Hangzhou 310027, People's Republic of China*
⁷¹*Zhengzhou University, Zhengzhou 450001, People's Republic of China*



(Received 31 January 2021; accepted 1 June 2021; published 6 July 2021)

Using data samples collected with the BESIII detector operating at the BEPCII storage ring at center-of-mass energies from 4.178 to 4.600 GeV, we study the process $e^+e^- \rightarrow \pi^0 X(3872)\gamma$ and search for

- ^aAlso at Bogazici University, 34342 Istanbul, Turkey
^bAlso at the Moscow Institute of Physics and Technology, Moscow 141700, Russia
^cAlso at the Novosibirsk State University, Novosibirsk, 630090, Russia
^dAlso at the NRC “Kurchatov Institute”, PNPI, 188300, Gatchina, Russia
^eAlso at Istanbul Arel University, 34295 Istanbul, Turkey
^fAlso at Goethe University Frankfurt, 60323 Frankfurt am Main, Germany
^gAlso at Key Laboratory for Particle Physics, Astrophysics and Cosmology, Ministry of Education; Shanghai Key Laboratory for Particle Physics and Cosmology; Institute of Nuclear and Particle Physics, Shanghai 200240, People's Republic of China
^hAlso at Key Laboratory of Nuclear Physics and Ion-beam Application (MOE) and Institute of Modern Physics, Fudan University, Shanghai 200443, People's Republic of China
ⁱAlso at Harvard University, Department of Physics, Cambridge, Massachusetts 02138, USA
^jCurrently at: Institute of Physics and Technology, Peace Ave.54B, Ulaanbaatar 13330, Mongolia
^kAlso at State Key Laboratory of Nuclear Physics and Technology, Peking University, Beijing 100871, People's Republic of China
^lSchool of Physics and Electronics, Hunan University, Changsha 410082, China
^mAlso at Guangdong Provincial Key Laboratory of Nuclear Science, Institute of Quantum Matter, South China Normal University, Guangzhou 510006, China

Published by the American Physical Society under the terms of the [Creative Commons Attribution 4.0 International license](https://creativecommons.org/licenses/by/4.0/). Further distribution of this work must maintain attribution to the author(s) and the published article's title, journal citation, and DOI. Funded by SCOAP³.

$Z_c(4020)^0 \rightarrow X(3872)\gamma$. We find no significant signal and set upper limits on $\sigma(e^+e^- \rightarrow \pi^0 X(3872)\gamma) \cdot \mathcal{B}(X(3872) \rightarrow \pi^+\pi^- J/\psi)$ and $\sigma(e^+e^- \rightarrow \pi^0 Z_c(4020)^0) \cdot \mathcal{B}(Z_c(4020)^0 \rightarrow X(3872)\gamma) \cdot \mathcal{B}(X(3872) \rightarrow \pi^+\pi^- J/\psi)$ for each energy point at 90% confidence level, which is of the order of several tenths pb.

DOI: 10.1103/PhysRevD.104.012001

I. INTRODUCTION

The recent discovery of several charmoniumlike states has attracted great experimental and theoretical interests [1]. The charmoniumlike states are also called XYZ states where X is the isospin-singlet state with $J^{PC} \neq 1^{--}$, Y is the isospin-singlet state with $J^{PC} = 1^{--}$, and Z is the isospin-triplet state [2]. The masses of these states are above the open-charm thresholds, and due to the unexpected resonance parameters and decay channels, these states cannot be described by conventional quark models. Therefore, they are good candidates for exotic states, such as hybrids, tetraquarks, molecules, etc. [3–5].

The first charmoniumlike state $X(3872)$, which has been recently renamed as $\chi_{c1}(3872)$ by the Particle Data Group (PDG [1]), was observed by the Belle experiment in the process $B^\pm \rightarrow K^\pm X(3872) \rightarrow K^\pm \pi^+ \pi^- J/\psi$ [6]. The $X(3872)$ is a rather narrow state with a mass that is consistent with $D^0 \bar{D}^{*0}$ threshold. It decays through open-charm, radiative and isospin-violating pion emission decays, and is found to be an isospin singlet with $J^{PC} = 1^{++}$ [1]. Among these features, the extremely small mass difference between the $X(3872)$ and $D^0 \bar{D}^{*0}$ threshold which we will denote as δ , is of particular interest. Taking the values for the D^0 , D^{*0} and $X(3872)$ masses from the PDG [1], δ is calculated to be (-10 ± 180) keV/ c^2 . Very recently, the LHCb reported a new measurement yielding $\delta = (70 \pm 120)$ keV/ c^2 [7,8]. However the improved precision is still insufficient to tell whether the $X(3872)$ mass is above or below the $D^0 \bar{D}^{*0}$ threshold. Better knowledge of δ will be an important step towards a deeper understanding of the nature of the $X(3872)$ [9,10], and eventually of other related XYZ states. A completely new method to measure the δ value by measuring the $X(3872)\gamma$ line shape, which is sensitive to the δ value due to a triangle singularity, is proposed by Refs. [11–13]. Here, the $X(3872)\gamma$ needs to be produced associated with another positive C -parity neutral meson, e.g., $e^+e^- \rightarrow \pi^0 X(3872)\gamma$. In principle, this method could be applied at the BESIII experiment, based on the sizable data samples taken for XYZ studies. According to the theoretical prediction in Ref. [13], the cross section of the process $e^+e^- \rightarrow \pi^0 X(3872)\gamma$ is expected to be small. However, there could be other scenarios where the expected cross section is large.

Recently, the BESIII Collaboration reported an enhancement around 4.2 GeV for the $e^+e^- \rightarrow \gamma X(3872)$ production cross sections [14], which suggests a connection between Y and X states. BESIII also reported another

connection, now between Y and Z states, with the observation of a $Y(4220)$ resonance in the process $e^+e^- \rightarrow \pi^0 Z_c(3900)^0$ [15]. Those observations may indicate some common nature among the XYZ states. Therefore, it is important to search for possible connections between Z and X states. Establishing connections among XYZ states may be a clue that can facilitate a better theoretical interpretation of these. One such connection [16] could be a transition $Z_c(4020)^0 \rightarrow X(3872)\gamma$ in the scenario where the $X(3872)$ is dominantly an S -wave $D^0 \bar{D}^{*0}$ molecule and the $Z_c(4020)^0$ is an isotopic triplet of near-threshold S -wave $D^* \bar{D}^*$ resonances. Therefore, the search for the transition $Z_c(4020)^0 \rightarrow X(3872)\gamma$ will help to quantitatively study the molecular picture of the $X(3872)$. The $Z_c(4020)$ is observed in the $e^+e^- \rightarrow \pi Z_c(4020)$ process, so the study of $e^+e^- \rightarrow \pi^0 X(3872)\gamma$ allows one to search for the transition $Z_c(4020)^0 \rightarrow X(3872)\gamma$.

In this paper, we report the search for the reaction $e^+e^- \rightarrow \pi^0 X(3872)\gamma$ and $Z_c(4020)^0 \rightarrow X(3872)\gamma$ based on the data of twenty-three energy points recorded with the BESIII detector in the range of $4.178 \leq \sqrt{s} \leq 4.600$ GeV. The $X(3872)$ state is reconstructed via $X(3872) \rightarrow \pi^+\pi^- J/\psi$, $J/\psi \rightarrow \ell^+\ell^-$ ($\ell = e$ or μ).

II. BESIII DETECTOR AND MONTE CARLO SIMULATION

The BESIII detector is a magnetic spectrometer [17] located at the Beijing Electron Positron Collider (BEPCII) [18]. The cylindrical core of the BESIII detector consists of a helium-based multilayer drift chamber (MDC), a plastic scintillator time-of-flight system (TOF), and a CsI(Tl) electromagnetic calorimeter (EMC), which are all enclosed in a superconducting solenoidal magnet, providing a 1.0 T magnetic field. The solenoid is supported by an octagonal flux-return yoke with resistive plate chamber muon identifier modules interleaved with steel. The acceptance of charged particles and photons is 93% over the 4π solid angle. The charged-particle momentum resolution at 1 GeV/ c is 0.5%, and the dE/dx resolution is 6% for the electrons from Bhabha scattering. The EMC measures photon energies with a resolution of 2.5% (5%) at 1 GeV in the barrel (end cap) region. The time resolution of the TOF barrel section is 68 ps, while that of the end cap section is 110 ps. The end cap TOF system was upgraded in 2015 with multigap resistive plate chamber technology, providing a time resolution of 60 ps [19]. About 70% of the data sample used here was taken after this upgrade.

Simulated data samples produced with the GEANT4-based [20] Monte Carlo (MC) package, which includes the geometric description of the BESIII detector and the detector response, are used to determine the detection efficiency and to estimate the background contributions. The simulation includes the beam energy spread and initial-state radiation (ISR) in the e^+e^- annihilations modeled with the generator KKMC [21]. The ISR production of vector charmonium(like) states and the continuum processes are incorporated also in KKMC [21]. The known decay modes are modeled with EVTGen [22], using branching fractions summarized and averaged by the PDG [1], and the remaining unknown decays from the charmonium states are generated with LUNDCHARM [23]. Final state radiation from charged final state particles is incorporated with the PHOTOS package [24].

Signal MC samples for $e^+e^- \rightarrow \pi^0 X(3872)\gamma$ and $e^+e^- \rightarrow \pi^0 Z_c(4020)^0 \rightarrow \pi^0 X(3872)\gamma$ are generated according to phase space at each center-of-mass energy point, assuming that the cross section follows the function fit for the $e^+e^- \rightarrow \pi^+\pi^-h_c$ line shape in Ref. [25]. The event selection criteria and the detection efficiencies are determined and studied based on signal MC samples of 1×10^5 signal events generated for each value of \sqrt{s} . Detection efficiencies are determined by the ratio of the reconstructed event yields (after the selection criteria) and the number of generated events. Inclusive MC samples consisting of open charm production processes are employed to investigate potential backgrounds.

III. EVENT SELECTION

For each charged track, the distance of closest approach to the interaction point (IP) is required to be within 10 cm in the beam direction and within 1 cm in the plane perpendicular to the beam direction. The polar angles (θ) of the tracks with respect to the beam axis (ignoring the small crossing angle), must be within the fiducial volume of the MDC ($|\cos\theta| < 0.93$). Photons are reconstructed from isolated showers in the EMC, which are at least 10° away from the nearest charged track. The photon energy is required to be at least 25 MeV in the barrel region ($|\cos\theta| < 0.80$) or 50 MeV in the end cap region ($0.86 < |\cos\theta| < 0.92$). To suppress electronic noise and energy depositions unrelated to the event, the EMC cluster timing from the reconstructed event start time is further required to satisfy $0 \leq t \leq 700$ ns.

Since the reaction $e^+e^- \rightarrow \pi^0 X(3872)\gamma$ results in the final states $\gamma\gamma\pi^+\pi^-\ell^+\ell^-$, candidate events are required to have four tracks with zero net charge and at least three photons. Tracks with momenta larger than 1.0 GeV/c are assigned as leptons from the J/ψ decay; otherwise, they are regarded as pions. Leptons from the J/ψ decay with energy deposited in the EMC larger than 1.0 GeV are identified as electrons, while those with less than 0.4 GeV as muons. The

π^0 candidates are reconstructed from photon pairs with invariant mass in the range $110 < M_{\gamma\gamma} < 150$ MeV/c².

To reduce the background contributions and to improve the mass resolution, a five-constraint (5C) kinematic fit is performed. Four constraints come from the total initial four momentum of the colliding beams; the last one is from constraining the $M_{\gamma\gamma}$ invariant mass to the nominal π^0 value [1]. If there is more than one combination in an event, the one with the smallest χ_{5C}^2 is chosen. Furthermore, the χ_{5C}^2 is required to be less than 60. The J/ψ is reconstructed via $\ell^+\ell^-$ decays, and the invariant mass of lepton pairs is required to be in the J/ψ mass window [3.080, 3.120] GeV/c².

IV. BORN CROSS SECTION MEASUREMENT

A. $e^+e^- \rightarrow \pi^0 X(3872)\gamma$

After applying the above requirements, the remaining background is mainly coming from $e^+e^- \rightarrow \gamma_{\text{ISR}}\eta J/\psi$, $\eta \rightarrow \pi^+\pi^-\pi^0$ and $e^+e^- \rightarrow \gamma\omega J/\psi$, $\omega \rightarrow \pi^+\pi^-\pi^0$ events. In order to veto these events, the $\pi^+\pi^-\pi^0$ invariant mass is required to be outside the η and ω mass regions [0.535, 0.560] GeV/c² and [0.750, 0.810] GeV/c², respectively. Besides the η and ω backgrounds, the $\pi^+\pi^-\psi(3686)$, $\psi(3686) \rightarrow \pi^0\pi^0 J/\psi$ background is removed by requiring the $\pi^+\pi^-$ recoil mass to be outside the $\psi(3686)$ mass region of [3.670, 3.700] GeV/c².

Figure 1 shows distributions of the $\pi^+\pi^-J/\psi$ invariant mass $M(\pi^+\pi^-J/\psi)$ for data and the MC samples of $e^+e^- \rightarrow \pi^0 X(3872)\gamma$. The $X(3872)$ signal region is taken as [3.860, 3.885] GeV/c², while the sideband regions are set to be [3.825, 3.850] GeV/c² and [3.895, 3.920] GeV/c². No significant $X(3872)$ signals are seen at any energies. The signal yield is determined from the event yields in the $X(3872)$ signal and sideband regions. The sideband yields are scaled by the ratio of the relevant mass-window widths in order to predict the background expected in the signal region. Upper limits on the number of signal events at the 90% C.L. are calculated by using a frequentist method [26] with unbounded profile likelihood treatment of systematic uncertainties, which is implemented by the package TROLKE [27] in the ROOT framework [28], where the signal and background obey Poisson statistics, and the efficiencies are Gaussian-distributed. The numerical results are summarized in Table I.

The Born cross section multiplied by the branching fraction $\sigma(e^+e^- \rightarrow \pi^0 X(3872)\gamma) \cdot \mathcal{B}(X(3872) \rightarrow \pi^+\pi^-J/\psi)$ is calculated as:

$$\begin{aligned} & \sigma(e^+e^- \rightarrow \pi^0 X(3872)\gamma) \cdot \mathcal{B}(X(3872) \rightarrow \pi^+\pi^-J/\psi) \\ &= \frac{N_{X(3872)}}{\epsilon \mathcal{L}_{\text{int}}(1 + \delta(s)) \frac{1}{|1 - \Pi|^2} \mathcal{B}(J/\psi \rightarrow \ell^+\ell^-) \mathcal{B}(\pi^0 \rightarrow \gamma\gamma)}, \quad (1) \end{aligned}$$

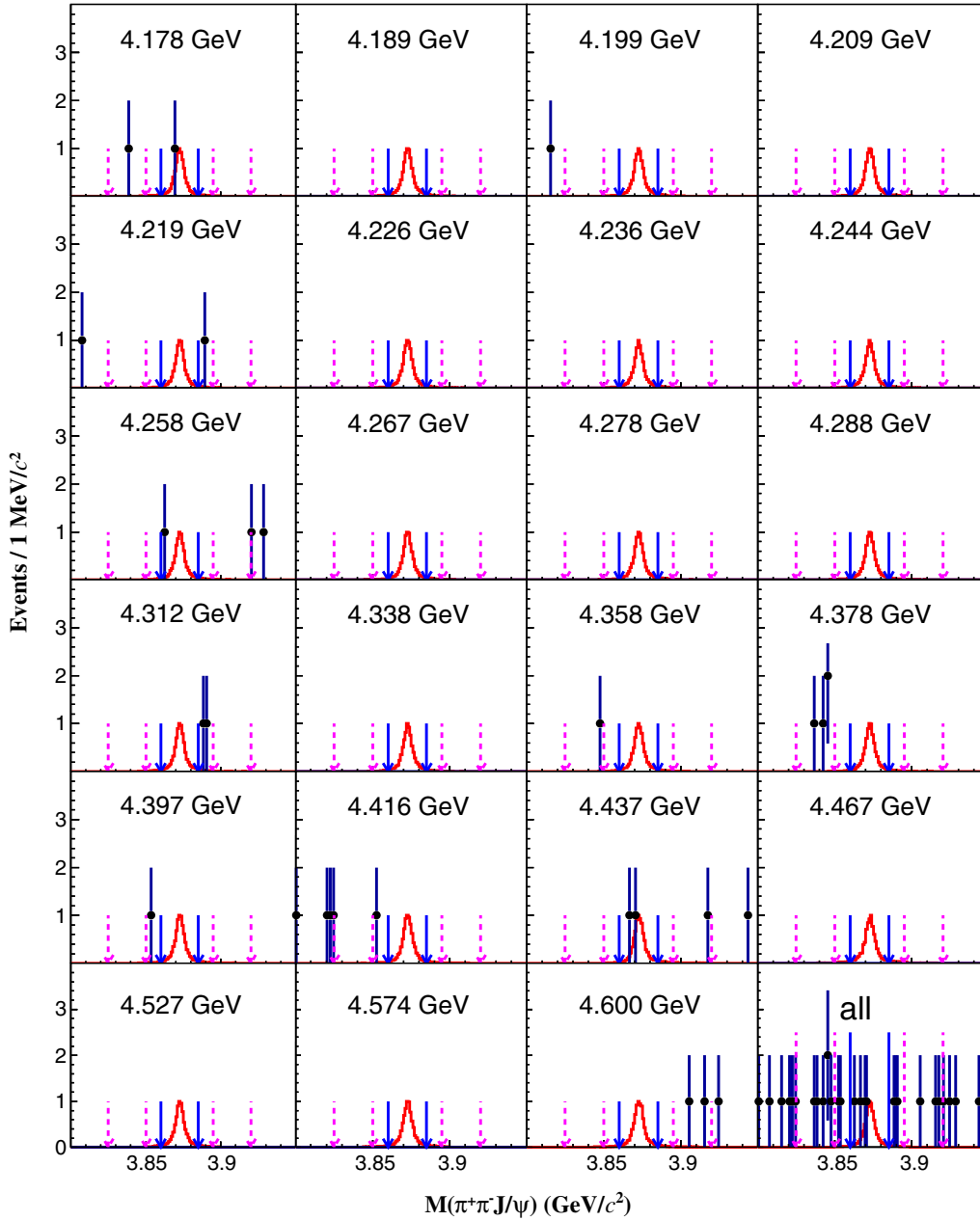


FIG. 1. The distribution of $M(\pi^+\pi^-J/\psi)$ for each energy point and the sum (all). Dots with error bars denote data, and the red histogram denotes the MC simulation of $e^+e^- \rightarrow \pi^0 X(3872)\gamma$. The blue solid lines mark the signal region of $X(3872)$, and the pink dashed lines mark the sideband regions of $X(3872)$.

where $N_{X(3872)}$ is the number of $X(3872)$ signal events, ϵ is the detection efficiency (excluding intermediate branching fractions), \mathcal{L}_{int} is the integrated luminosity [29], $1 + \delta(s)$ is the ISR correction factor obtained from a quantum electrodynamics calculations [21,30], $\frac{1}{|1-\Pi|^2}$ is vacuum polarization factor [31]. The corresponding upper limits for this cross section at the 90% C.L. for each energy point are listed in Table I and shown in Fig. 2(a).

Assuming the Born cross section of $e^+e^- \rightarrow \pi^0 X(3872)\gamma$ is constant at $4.178 \leq \sqrt{s} \leq 4.600$ GeV, the

average Born cross section multiplied by the branching fraction $\bar{\sigma}(e^+e^- \rightarrow \pi^0 X(3872)\gamma) \cdot \mathcal{B}(X(3872) \rightarrow \pi^+\pi^-J/\psi)$ for data is calculated as:

$$\begin{aligned} & \bar{\sigma}(e^+e^- \rightarrow \pi^0 X(3872)\gamma) \cdot \mathcal{B}(X(3872) \rightarrow \pi^+\pi^-J/\psi) \\ &= \frac{N_{X(3872)}^{\text{total}}}{\sum_i (\epsilon \mathcal{L}_{\text{int}} (1 + \delta(s)) \frac{1}{|1-\Pi|^2})_i \mathcal{B}(J/\psi \rightarrow \ell^+\ell^-) \mathcal{B}(\pi^0 \rightarrow \gamma\gamma)}, \end{aligned} \quad (2)$$

TABLE I. The upper limits (calculated including the systematic uncertainties) on $\sigma(e^+e^- \rightarrow \pi^0 X(3872)\gamma) \cdot \mathcal{B}(X(3872) \rightarrow \pi^+\pi^- J/\psi)$ and $\sigma(e^+e^- \rightarrow \pi^0 Z_c(4020)^0) \cdot \mathcal{B}(Z_c(4020)^0 \rightarrow X(3872)\gamma) \cdot \mathcal{B}(X(3872) \rightarrow \pi^+\pi^- J/\psi)$ at the 90% C.L. for each energy point, together with integrated luminosities \mathcal{L}_{int} , the number of events in signal region N^{obs} , the number of events in sideband region N^{sb} , the number of signal events N at the 90% C.L., radiative correction factors $1 + \delta(s)$, vacuum polarization factors $\frac{1}{|1-\Pi|^2}$, and efficiencies without intermediate branching fractions ϵ . Here, $\sigma \cdot \mathcal{B}$ represents $\sigma(e^+e^- \rightarrow \pi^0 X(3872)\gamma) \cdot \mathcal{B}(X(3872) \rightarrow \pi^+\pi^- J/\psi)$ or $\sigma(e^+e^- \rightarrow \pi^0 Z_c(4020)^0) \cdot \mathcal{B}(Z_c(4020)^0 \rightarrow X(3872)\gamma) \cdot \mathcal{B}(X(3872) \rightarrow \pi^+\pi^- J/\psi)$. The first values in brackets are for the process $e^+e^- \rightarrow \pi^0 X(3872)\gamma$, and the second for the process $e^+e^- \rightarrow \pi^0 Z_c(4020)^0 \rightarrow \pi^0 X(3872)\gamma$. The low efficiency at 4.467 GeV is caused by the cut on the $\pi^+\pi^-$ recoil mass.

\sqrt{s} (GeV)	\mathcal{L}_{int} (pb $^{-1}$)	N^{obs}	N^{sb}	N	$1 + \delta(s)$	$\frac{1}{ 1-\Pi ^2}$	ϵ (%)	$\sigma \cdot \mathcal{B}$ (pb)
4.178	3195	(1, 0)	(1, 1)	(< 3.27, < 1.26)	(0.70, 0.69)	1.055	(14.02, 13.97)	(< 0.08, < 0.03)
4.189	527	(0, 0)	(0, 2)	(< 2.00, < 0.52)	(0.70, 0.70)	1.056	(14.12, 14.02)	(< 0.31, < 0.08)
4.199	526	(0, 0)	(0, 0)	(< 2.00, < 2.00)	(0.70, 0.70)	1.057	(14.13, 14.24)	(< 0.31, < 0.31)
4.209	517	(0, 0)	(0, 0)	(< 2.00, < 2.00)	(0.71, 0.71)	1.057	(14.29, 13.75)	(< 0.31, < 0.32)
4.219	515	(0, 0)	(0, 0)	(< 2.00, < 2.00)	(0.72, 0.72)	1.057	(14.07, 13.74)	(< 0.31, < 0.31)
4.226	1056	(0, 0)	(0, 0)	(< 2.00, < 2.00)	(0.74, 0.74)	1.057	(14.51, 14.11)	(< 0.14, < 0.15)
4.236	530	(0, 0)	(0, 0)	(< 1.99, < 2.00)	(0.76, 0.76)	1.056	(14.50, 13.43)	(< 0.27, < 0.30)
4.244	538	(0, 0)	(0, 0)	(< 2.00, < 2.00)	(0.78, 0.78)	1.056	(14.03, 13.20)	(< 0.27, < 0.29)
4.258	828	(1, 0)	(0, 0)	(< 3.69, < 2.01)	(0.81, 0.81)	1.054	(14.00, 12.99)	(< 0.32, < 0.19)
4.267	531	(0, 0)	(0, 0)	(< 2.00, < 2.01)	(0.83, 0.83)	1.053	(13.78, 12.23)	(< 0.27, < 0.30)
4.278	176	(0, 0)	(0, 0)	(< 2.00, < 2.02)	(0.84, 0.84)	1.053	(13.44, 11.89)	(< 0.81, < 0.93)
4.288	502	(0, 0)	(0, 0)	(< 2.00, < 2.01)	(0.84, 0.84)	1.053	(13.29, 11.74)	(< 0.29, < 0.33)
4.312	501	(0, 0)	(0, 0)	(< 2.00, < 2.02)	(0.84, 0.84)	1.052	(13.35, 11.68)	(< 0.29, < 0.33)
4.338	505	(0, 0)	(0, 0)	(< 2.00, < 2.02)	(0.83, 0.83)	1.051	(13.76, 12.03)	(< 0.28, < 0.32)
4.358	544	(0, 0)	(1, 0)	(< 1.57, < 2.02)	(0.83, 0.83)	1.051	(14.11, 12.42)	(< 0.20, < 0.29)
4.378	523	(0, 0)	(4, 0)	(< 0.30, < 2.02)	(0.84, 0.84)	1.052	(14.06, 12.47)	(< 0.04, < 0.30)
4.397	508	(0, 0)	(0, 0)	(< 2.00, < 2.02)	(0.86, 0.86)	1.052	(13.60, 12.34)	(< 0.27, < 0.30)
4.416	1044	(0, 0)	(0, 0)	(< 2.00, < 2.03)	(0.90, 0.90)	1.053	(13.04, 12.10)	(< 0.13, < 0.14)
4.437	570	(2, 0)	(1, 1)	(< 4.93, < 1.57)	(0.97, 0.97)	1.054	(9.94, 11.47)	(< 0.72, < 0.20)
4.467	111	(0, 0)	(0, 0)	(< 2.00, < 2.03)	(1.09, 1.09)	1.055	(5.25, 10.39)	(< 2.53, < 1.30)
4.527	112	(0, 0)	(0, 0)	(< 2.00, < 2.02)	(1.38, 1.38)	1.055	(9.19, 8.56)	(< 1.13, < 1.23)
4.574	49	(0, 0)	(0, 0)	(< 2.00, < 2.03)	(1.62, 1.62)	1.055	(8.11, 7.31)	(< 2.50, < 2.81)
4.600	587	(0, 0)	(2, 0)	(< 1.15, < 2.02)	(1.76, 1.75)	1.055	(7.71, 7.06)	(< 0.12, < 0.22)

where $N_{X(3872)}^{\text{total}}$ is the total number of $X(3872)$ signal events, and i denotes each energy point. The corresponding upper limit for the average Born cross section multiplied by the branching fraction is determined to be 21.9 fb at the 90% C.L.

B. $Z_c(4020)^0 \rightarrow X(3872)\gamma$

The possible connection between X and Z charmonium-like states can be studied via the decay $Z_c(4020)^0 \rightarrow X(3872)\gamma$. In order to search for the process, the $X(3872)$ signal region is set to be $[3.860, 3.885]$ GeV/ c^2 , which is the

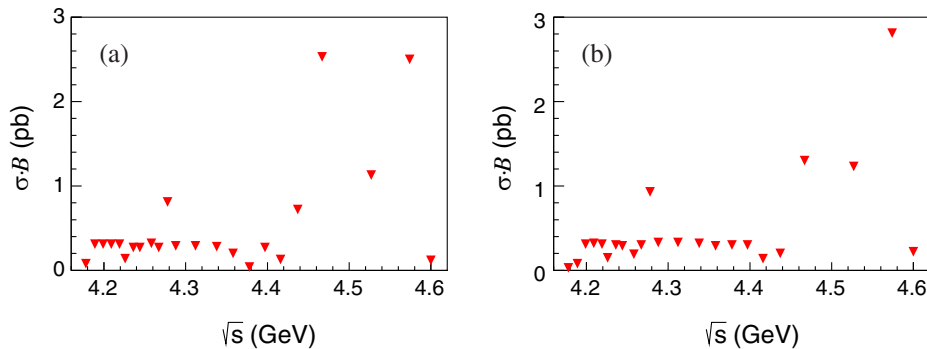


FIG. 2. The upper limits at the 90% C.L. on $\sigma(e^+e^- \rightarrow \pi^0 X(3872)\gamma) \cdot \mathcal{B}(X(3872) \rightarrow \pi^+\pi^- J/\psi)$ (a) and $\sigma(e^+e^- \rightarrow \pi^0 Z_c(4020)^0) \cdot \mathcal{B}(Z_c(4020)^0 \rightarrow X(3872)\gamma) \cdot \mathcal{B}(X(3872) \rightarrow \pi^+\pi^- J/\psi)$ (b) for each energy point.

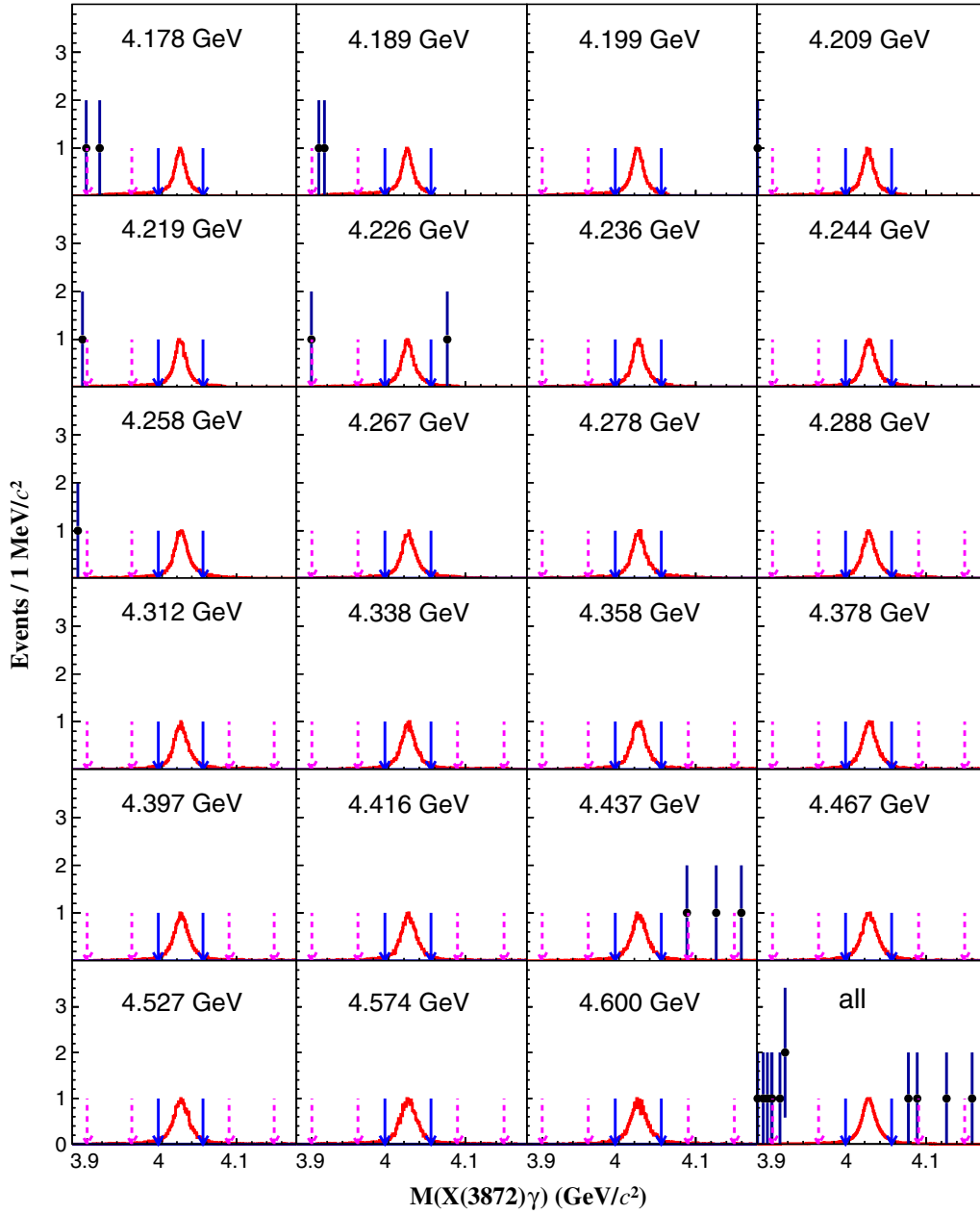


FIG. 3. The distribution of $M(X(3872)\gamma)$ for each energy point and the sum (all). Dots with error bars denote data, and the red histogram denotes the MC simulation of $e^+e^- \rightarrow \pi^0 Z_c(4020)^0 \rightarrow \pi^0 X(3872)\gamma$. The blue solid lines mark the signal region of $Z_c(4020)^0$, and the pink dashed lines mark the sideband regions of $Z_c(4020)^0$.

same as for the $e^+e^- \rightarrow \pi^0 X(3872)\gamma$ study. As we do not observe any $X(3872)$ signal, there cannot be any $Z_c(4020)^0$ being produced in the given channel. Still, we provide corresponding upper limits, since a quantification might well be helpful in the understanding of the involved states. After the requirement of the $X(3872)$ mass window no significant η , ω and $\psi(3686)$ background remain. Figure 3 shows the $X(3872)\gamma$ invariant mass distributions for data and MC samples of $e^+e^- \rightarrow \pi^0 Z_c(4020)^0 \rightarrow \pi^0 X(3872)\gamma$. No $Z_c(4020)^0$ candidates are found. Therefore, the

same method as before is employed to calculate the upper limits for this process. For data samples taken above $\sqrt{s} = 4.280$ GeV, the $Z_c(4020)^0$ signal region is set to be $[3.995, 4.055]$ GeV/c^2 , and the sideband regions are set to be $[3.900, 3.960]$ GeV/c^2 and $[4.090, 4.150]$ GeV/c^2 . At lower energies, kinematics dictates that $Z_c(4020)^0$ candidates cannot have a mass above $4.28 - M_{\pi^0} = 4.145$ GeV/c^2 , where M_{π^0} is π^0 nominal mass. Accordingly, we use a single sideband region of $[3.900, 3.960]$ GeV/c^2 .

The Born cross section multiplied by branching fractions $\sigma(e^+e^- \rightarrow \pi^0 Z_c(4020)^0) \cdot \mathcal{B}(Z_c(4020)^0 \rightarrow X(3872)\gamma) \cdot \mathcal{B}(X(3872) \rightarrow \pi^+\pi^- J/\psi)$ is calculated with the following formula:

$$\begin{aligned} & \sigma(e^+e^- \rightarrow \pi^0 Z_c(4020)^0) \cdot \mathcal{B}(Z_c(4020)^0 \rightarrow X(3872)\gamma) \\ & \cdot \mathcal{B}(X(3872) \rightarrow \pi^+\pi^- J/\psi) \\ & = \frac{N_{Z_c(4020)^0}}{\epsilon \mathcal{L}_{\text{int}}(1 + \delta(s)) \frac{1}{|1 - \Pi|^2} \mathcal{B}(J/\psi \rightarrow \ell^+ \ell^-) \mathcal{B}(\pi^0 \rightarrow \gamma\gamma)}, \quad (3) \end{aligned}$$

where $N_{Z_c(4020)^0}$ is the number of $Z_c(4020)^0$ signal events. The corresponding upper limits at the 90% C.L. for each energy are listed in Table I and shown in Fig. 2(b).

Assuming the Born cross section of $e^+e^- \rightarrow \pi^0 Z_c(4020)^0$ is constant at $4.178 \leq \sqrt{s} \leq 4.600$ GeV, the average Born cross section multiplied by branching fractions $\bar{\sigma}(e^+e^- \rightarrow \pi^0 Z_c(4020)^0) \cdot \mathcal{B}(Z_c(4020)^0 \rightarrow X(3872)\gamma) \cdot \mathcal{B}(X(3872) \rightarrow \pi^+\pi^- J/\psi)$ for data is calculated with the following formula:

$$\begin{aligned} & \bar{\sigma}(e^+e^- \rightarrow \pi^0 Z_c(4020)^0) \cdot \mathcal{B}(Z_c(4020)^0 \rightarrow X(3872)\gamma) \\ & \cdot \mathcal{B}(X(3872) \rightarrow \pi^+\pi^- J/\psi) \\ & = \frac{N_{Z_c(4020)^0}^{\text{total}}}{\sum_i (\epsilon \mathcal{L}_{\text{int}}(1 + \delta(s)) \frac{1}{|1 - \Pi|^2})_i \mathcal{B}(J/\psi \rightarrow \ell^+ \ell^-) \mathcal{B}(\pi^0 \rightarrow \gamma\gamma)}, \quad (4) \end{aligned}$$

where $N_{Z_c(4020)^0}^{\text{total}}$ is the total number of $Z_c(4020)^0$ signal events. The corresponding upper limit for the average Born cross section multiplied by the branching fraction is determined to be 1.6 fb at the 90% C.L.

V. SYSTEMATIC UNCERTAINTY ESTIMATION

The systematic uncertainties of $\sigma(e^+e^- \rightarrow \pi^0 X(3872)\gamma) \cdot \mathcal{B}(X(3872) \rightarrow \pi^+\pi^- J/\psi)$ and $\sigma(e^+e^- \rightarrow \pi^0 Z_c(4020)^0) \cdot \mathcal{B}(Z_c(4020)^0 \rightarrow X(3872)\gamma) \cdot \mathcal{B}(X(3872) \rightarrow \pi^+\pi^- J/\psi)$ originate from the luminosity measurement, the tracking efficiency, the photon detection efficiency, the kinematic fit, the J/ψ mass window, the $X(3872)$ mass window, the $Z_c(4020)^0$ parameters, the line shape, the generator model, the ISR correction, and the input branching fractions.

The integrated luminosity at each point has been measured with a precision of 1.0% using the Bhabha process [29].

The uncertainty from the tracking efficiency is 1.0% per track [32] and the uncertainty in photon detection efficiency is 1.0% per photon [33].

The uncertainty due to the kinematic fit requirements is estimated by correcting the helix parameters of charged tracks according to the method described in Ref. [34]. The difference between detection efficiencies obtained from

MC samples with and without this correction is taken as the uncertainty.

The uncertainty for the J/ψ mass window is estimated using the control sample of $e^+e^- \rightarrow \gamma_{\text{ISR}}\psi(3686)$, $\psi(3686) \rightarrow \pi^+\pi^- J/\psi$. The difference of the efficiency between data and MC simulation is found to be 1.6% [35], which is taken as the uncertainty.

The uncertainty from the $X(3872)$ mass window is estimated by changing the window range by $\pm 10\%$, and the largest efficiency change is taken as the uncertainty.

The uncertainties arising from the $Z_c(4020)^0$ mass and width are estimated by changing them by one standard deviation values [1] while generating the signal MC. The largest efficiency difference relative to the nominal one is taken as the uncertainty.

The line shape affects the ISR correction factor and the efficiency. No obvious signal was found for our $Z_c(4020)^0$ search, so we use the line shape from $e^+e^- \rightarrow \pi^+\pi^- h_c$ in Ref. [25] as the input line shape to get the nominal results. To get the uncertainty introduced by the line shape, we change it to a Breit-Wigner function describing the $\psi(4230)$ or $\psi(4415)$, with the masses and widths fixed to the values from PDG [1]. The largest difference of the final result is taken as a systematic uncertainty.

For the systematic uncertainty from the MC simulation describing the process $e^+e^- \rightarrow \pi^0 X(3872)\gamma$, we use the three-body phase space MC simulation to get the nominal efficiency, then change to the $e^+e^- \rightarrow \pi^0 Z_c(4020)^0 \rightarrow \pi^0 X(3872)\gamma$. The difference on the detection efficiency with and without the intermediate resonant state is taken as the uncertainty due to the MC generator model.

The systematic uncertainty from the MC simulation describing the process $e^+e^- \rightarrow \pi^0 Z_c(4020)^0 \rightarrow \pi^0 X(3872)\gamma$ is estimated by varying the distribution of the π^0 polar angle θ . The nominal efficiency is determined assuming a flat distribution in $\cos\theta$. A conservative estimate of the systematic uncertainty is obtained using alternative MC samples with angular distributions of $1 \pm \cos^2\theta$. The largest change of efficiency is taken as the uncertainty due to the MC generator model.

The ISR correction factor is obtained from quantum electrodynamics calculations [21,30]. We also analyze MC samples with and without ISR effects considered to get the ISR correction factor, the difference of the two results is taken as the systematic uncertainty on the ISR correction factor.

As uncertainties introduced by the branching fractions of $J/\psi \rightarrow \ell^+ \ell^-$ and $\pi^0 \rightarrow \gamma\gamma$ we use those quoted by the PDG [1].

Table II summarizes all the systematic uncertainties related to $\sigma(e^+e^- \rightarrow \pi^0 X(3872)\gamma) \cdot \mathcal{B}(X(3872) \rightarrow \pi^+\pi^- J/\psi)$ and $\sigma(e^+e^- \rightarrow \pi^0 Z_c(4020)^0) \cdot \mathcal{B}(Z_c(4020)^0 \rightarrow X(3872)\gamma) \cdot \mathcal{B}(X(3872) \rightarrow \pi^+\pi^- J/\psi)$ for each center-of-mass energy. The total systematic uncertainty for each energy point is

TABLE II. Summary of relative systematic uncertainties (%) associated with luminosity (\mathcal{L}_{int}), tracking efficiency (Tracks), photon detection efficiency (Photons), kinematic fitting (χ_{5C}^2), J/ψ mass window (J/ψ), $X(3872)$ mass window ($X(3872)$), $Z_c(4020)^0$ parameters ($Z_c(4020)^0$), line shape (Line shape), generator model (Generator), ISR correction factor (ISR) and branching fraction (\mathcal{B}). The first values in brackets are for the process $e^+e^- \rightarrow \pi^0 X(3872)\gamma$, and the second for the process $e^+e^- \rightarrow \pi^0 Z_c(4020)^0 \rightarrow \pi^0 X(3872)\gamma$. A dash indicates that a systematic effect is not applicable.

\sqrt{s} (GeV)	\mathcal{L}_{int}	Tracks	Photons	χ_{5C}^2	J/ψ	$X(3872)$	$Z_c(4020)^0$	Line shape	Generator	ISR	\mathcal{B}	Sum
4.178	1.0	4.0	3.0	(2.6, 2.0)	1.6	1.3	(-, 4.2)	(5.6, 6.0)	(7.4, 2.4)	(0.7, 0.7)	0.4	(11.1, 9.7)
4.189	1.0	4.0	3.0	(2.8, 2.1)	1.6	1.3	(-, 3.5)	(6.4, 6.8)	(5.7, 3.9)	(0.7, 0.6)	0.4	(10.6, 10.4)
4.199	1.0	4.0	3.0	(2.1, 2.2)	1.6	1.3	(-, 4.3)	(6.7, 4.7)	(7.5, 3.9)	(0.5, 0.5)	0.4	(11.7, 9.6)
4.209	1.0	4.0	3.0	(2.0, 2.1)	1.6	1.4	(-, 4.1)	(4.9, 6.3)	(3.5, 6.6)	(0.2, 0.3)	0.4	(8.4, 11.6)
4.219	1.0	4.0	3.0	(2.4, 2.6)	1.6	1.5	(-, 5.7)	(4.3, 3.5)	(5.2, 7.7)	(0.1, 0.1)	0.4	(9.1, 11.9)
4.226	1.0	4.0	3.0	(2.3, 2.1)	1.6	1.5	(-, 5.6)	(1.5, 2.3)	(5.1, 7.1)	(0.1, 0.1)	0.4	(8.0, 11.1)
4.236	1.0	4.0	3.0	(2.3, 2.1)	1.6	1.5	(-, 6.3)	(2.1, 2.2)	(1.3, 9.2)	(0.1, 0.1)	0.4	(6.5, 12.8)
4.244	1.0	4.0	3.0	(2.1, 2.3)	1.6	1.3	(-, 4.6)	(4.4, 1.3)	(3.3, 9.7)	(0.2, 0.1)	0.4	(8.1, 12.4)
4.258	1.0	4.0	3.0	(2.3, 2.6)	1.6	1.6	(-, 5.8)	(6.4, 4.4)	(3.3, 9.5)	(0.2, 0.3)	0.4	(9.4, 13.5)
4.267	1.0	4.0	3.0	(2.0, 2.0)	1.6	1.3	(-, 5.9)	(5.7, 6.8)	(0.2, 12.9)	(0.2, 0.1)	0.4	(8.2, 16.8)
4.278	1.0	4.0	3.0	(2.4, 2.1)	1.6	1.5	(-, 5.6)	(6.9, 7.2)	(1.0, 13.6)	(0.2, 0.1)	0.4	(9.2, 17.4)
4.288	1.0	4.0	3.0	(2.1, 2.2)	1.6	1.4	(-, 5.9)	(7.9, 6.0)	(1.3, 13.5)	(0.2, 0.1)	0.4	(10.0, 17.0)
4.312	1.0	4.0	3.0	(2.8, 2.1)	1.6	1.3	(-, 6.6)	(5.8, 5.9)	(2.2, 15.4)	(0.1, 0.2)	0.4	(8.8, 18.7)
4.338	1.0	4.0	3.0	(2.1, 2.2)	1.6	1.5	(-, 5.4)	(7.0, 5.6)	(2.9, 16.0)	(0.1, 0.1)	0.4	(9.6, 18.8)
4.358	1.0	4.0	3.0	(2.0, 1.8)	1.6	1.2	(-, 5.6)	(7.6, 6.1)	(2.8, 15.5)	(0.1, 0.1)	0.4	(10.0, 18.5)
4.378	1.0	4.0	3.0	(2.1, 1.8)	1.6	1.5	(-, 6.0)	(7.0, 3.9)	(3.5, 14.9)	(0.1, 0.1)	0.4	(9.8, 17.5)
4.397	1.0	4.0	3.0	(2.1, 1.8)	1.6	1.3	(-, 7.4)	(5.3, 5.5)	(5.3, 16.4)	(0.1, 0.1)	0.4	(9.5, 19.7)
4.416	1.0	4.0	3.0	(1.8, 1.7)	1.6	1.3	(-, 7.1)	(4.4, 5.5)	(4.3, 19.0)	(0.1, 0.1)	0.4	(8.5, 21.8)
4.437	1.0	4.0	3.0	(2.1, 2.0)	1.6	1.4	(-, 7.1)	(3.1, 1.2)	(5.9, 17.4)	(0.1, 0.2)	0.4	(8.9, 19.7)
4.467	1.0	4.0	3.0	(2.4, 2.2)	1.6	1.5	(-, 7.3)	(3.7, 5.5)	(9.8, 18.2)	(0.1, 0.1)	0.4	(12.1, 21.2)
4.527	1.0	4.0	3.0	(2.6, 1.5)	1.6	1.5	(-, 7.4)	(5.8, 2.1)	(5.5, 17.8)	(0.2, 0.3)	0.4	(10.1, 20.2)
4.575	1.0	4.0	3.0	(2.3, 1.5)	1.6	1.4	(-, 7.2)	(4.1, 3.0)	(7.4, 20.1)	(0.5, 0.5)	0.4	(10.4, 22.3)
4.600	1.0	4.0	3.0	(2.3, 1.9)	1.6	1.4	(-, 6.6)	(0.4, 1.1)	(8.1, 16.2)	(0.5, 0.6)	0.4	(10.1, 18.5)

calculated as the quadratic sum of the individual uncertainties, assuming them to be uncorrelated.

VI. SUMMARY

Using data samples collected at the center-of-mass energies between 4.178 and 4.600 GeV, the processes $e^+e^- \rightarrow \pi^0 X(3872)\gamma$ and $Z_c(4020)^0 \rightarrow X(3872)\gamma$ are investigated. In neither of the two processes are significant signals observed. Upper limits at the 90% C.L. on the cross sections multiplied by the branching fractions, $\sigma(e^+e^- \rightarrow \pi^0 X(3872)\gamma) \cdot \mathcal{B}(X(3872) \rightarrow \pi^+ \pi^- J/\psi)$ and $\sigma(e^+e^- \rightarrow \pi^0 Z_c(4020)^0) \cdot \mathcal{B}(Z_c(4020)^0 \rightarrow X(3872)\gamma) \cdot \mathcal{B}(X(3872) \rightarrow \pi^+ \pi^- J/\psi)$, are reported for each energy point. The average cross sections multiplied by branching fractions are also determined. The measured results of the process $e^+e^- \rightarrow \pi^0 X(3872)\gamma$ are not in conflict with the theoretical expectation of about 0.1 fb [13]. A three orders of magnitude increase in statistics is needed to test these models.

Using the experimental results on the $\sigma(e^+e^- \rightarrow \pi^0 Z_c(4020)^0) \cdot \mathcal{B}(Z_c(4020)^0 \rightarrow (D^* \bar{D}^*)^0)$ at $\sqrt{s} = 4.226$ and 4.258 GeV [36], the ratio $\frac{\mathcal{B}(Z_c(4020)^0 \rightarrow X(3872)\gamma) \cdot \mathcal{B}(X(3872) \rightarrow \pi^+ \pi^- J/\psi)}{\mathcal{B}(Z_c(4020)^0 \rightarrow (D^* \bar{D}^*)^0)}$ is determined to be less than 0.15% at the 90% C.L. The ratio does not contradict the prediction reported in Ref. [16] based on

the molecular picture. Since no significant $e^+e^- \rightarrow \pi^0 X(3872)\gamma$ signals are observed, we cannot study the lineshape as proposed in Refs. [11,12]; this may be achieved at future super tau-charm facilities [37,38].

ACKNOWLEDGMENTS

The BESIII collaboration thanks the staff of BEPCII and the IHEP computing center for their strong support. This work is supported in part by National Key Research and Development Program of China under Contracts No. 2020YFA0406300, No. 2020YFA0406400; National Natural Science Foundation of China (NSFC) under Contracts No. 11905179, No. 11625523, No. 11635010, No. 11735014, No. 11822506, No. 11835012, No. 11935015, No. 11935016, No. 11935018, No. 11961141012; the Chinese Academy of Sciences (CAS) Large-Scale Scientific Facility Program; Joint Large-Scale Scientific Facility Funds of the NSFC and CAS under Contracts No. U1732263, No. U1832207; CAS Key Research Program of Frontier Sciences under Contracts No. QYZDJ-SSW-SLH003, No. QYZDJ-SSW-SLH040; 100 Talents Program of CAS; INPAC and Shanghai Key Laboratory for Particle Physics and Cosmology; ERC under Contract No. 758462; European

Union Horizon 2020 research and innovation programme under Contract No. Marie Skłodowska-Curie Grant agreement No. 894790; Nanhu Scholars Program for Young Scholars of Xinyang Normal University; German Research Foundation DFG under Contracts Nos. 443159800, Collaborative Research Center CRC 1044, FOR 2359, FOR 2359, GRK 214; Istituto Nazionale di Fisica Nucleare, Italy; Ministry of Development of Turkey under

Contract No. DPT2006K-120470; National Science and Technology fund; Olle Engkvist Foundation under Contract No. 200-0605; STFC (United Kingdom); The Knut and Alice Wallenberg Foundation (Sweden) under Contract No. 2016.0157; The Royal Society, UK under Contracts No. DH140054, No. DH160214; The Swedish Research Council; U.S. Department of Energy under Contracts No. DE-FG02-05ER41374, No. DE-SC-0012069.

-
- [1] P. A. Zyla *et al.* (Particle Data Group), *Prog. Theor. Phys.* **2020**, 083C01 (2020).
- [2] M. Ablikim *et al.* (BESIII Collaboration), *Phys. Rev. Lett.* **108**, 232001 (2012).
- [3] N. Brambilla *et al.*, *Eur. Phys. J. C* **71**, 1534 (2011).
- [4] R. A. Briceno *et al.*, *Chin. Phys. C* **40**, 042001 (2016).
- [5] H. X. Chen, W. Chen, X. Liu, and S. L. Zhu, *Phys. Rep.* **639**, 1 (2016).
- [6] S. K. Choi *et al.* (Belle Collaboration), *Phys. Rev. Lett.* **91**, 262001 (2003).
- [7] R. Aaij *et al.* (LHCb Collaboration), *J. High Energy Phys.* **08** (2020) 123.
- [8] R. Aaij *et al.* (LHCb Collaboration), *Phys. Rev. D* **102**, 092005 (2020).
- [9] C. Hanhart, Y. S. Kalashnikova, A. E. Kudryavtsev, and A. V. Nefediev, *Phys. Rev. D* **76**, 034007 (2007).
- [10] P. Artoisenet, E. Braaten, and D. Kang, *Phys. Rev. D* **82**, 014013 (2010).
- [11] F. K. Guo, *Phys. Rev. Lett.* **122**, 202002 (2019).
- [12] P. G. Ortega and E. R. Arriola, [arXiv:2007.11608](https://arxiv.org/abs/2007.11608).
- [13] S. Sakai, H. J. Jing, and F. K. Guo, *Phys. Rev. D* **102**, 114041 (2020).
- [14] M. Ablikim *et al.* (BESIII Collaboration), *Phys. Rev. Lett.* **122**, 232002 (2019).
- [15] M. Ablikim *et al.* (BESIII Collaboration), *Phys. Rev. D* **102**, 012009 (2020).
- [16] M. B. Voloshin, *Phys. Rev. D* **99**, 054028 (2019).
- [17] M. Ablikim *et al.* (BESIII Collaboration), *Nucl. Instrum. Methods Phys. Res., Sect. A* **614**, 345 (2010); *Chin. Phys. C* **44**, 040001 (2020).
- [18] C. H. Yu *et al.*, *Proceedings of IPAC2016, Busan, Korea* (JACoW, Geneva, Switzerland, 2016), <https://doi.org/10.18429/JACoW-IPAC2016-TUYA01>.
- [19] X. Li *et al.*, *Rad. Det. Tech. Meth.* **1**, 13 (2017); Y. X. Guo *et al.*, *Rad. Det. Tech. Meth.* **1**, 15 (2017).
- [20] S. Agostinelli *et al.* (GEANT4 Collaboration), *Nucl. Instrum. Methods Phys. Res., Sect. A* **506**, 250 (2003).
- [21] S. Jadach, B. F. L. Ward, and Z. Was, *Phys. Rev. D* **63**, 113009 (2001); *Comput. Phys. Commun.* **130**, 260 (2000).
- [22] D. J. Lange, *Nucl. Instrum. Methods Phys. Res., Sect. A* **462**, 152 (2001); R. G. Ping, *Chin. Phys. C* **32**, 599 (2008).
- [23] J. C. Chen, G. S. Huang, X. R. Qi, D. H. Zhang, and Y. S. Zhu, *Phys. Rev. D* **62**, 034003 (2000); R. L. Yang, R. G. Ping, and H. Chen, *Chin. Phys. Lett.* **31**, 061301 (2014).
- [24] E. Richter-Was, *Phys. Lett. B* **303**, 163 (1993).
- [25] M. Ablikim *et al.* (BESIII Collaboration), *Phys. Rev. Lett.* **118**, 092002 (2017).
- [26] W. A. Rolke, A. M. Lopez, and J. Conrad, *Nucl. Instrum. Methods Phys. Res., Sect. A* **551**, 493 (2005).
- [27] <https://root.cern.ch/root/html604/TRolke.html>.
- [28] <https://root.cern/manual>.
- [29] M. Ablikim *et al.* (BESIII Collaboration), *Chin. Phys. C* **39**, 093001 (2015).
- [30] E. A. Kuraev and V. S. Fadin, *Sov. J. Nucl. Phys.* **41**, 466 (1985).
- [31] S. Actis *et al.* (Working Group on Radiative Corrections and Monte Carlo Generators for Low Energies), *Eur. Phys. J. C* **66**, 585 (2010).
- [32] M. Ablikim *et al.* (BESIII Collaboration), *Phys. Rev. D* **99**, 091103(R) (2019).
- [33] M. Ablikim *et al.* (BESIII Collaboration), *Phys. Rev. D* **101**, 012008 (2020).
- [34] M. Ablikim *et al.* (BESIII Collaboration), *Phys. Rev. D* **87**, 012002 (2013).
- [35] M. Ablikim *et al.* (BESIII Collaboration), *Phys. Rev. D* **93**, 011102(R) (2016); **103**, L091102 (2021).
- [36] M. Ablikim *et al.* (BESIII Collaboration), *Phys. Rev. Lett.* **115**, 182002 (2015).
- [37] A. E. Bondar *et al.* (Charm-Tau Factory Collaboration), *Phys. At. Nucl.* **76**, 1072 (2013).
- [38] Z. Zhou *et al.*, *Proceedings of the 7th International Particle Accelerator Conference (IPAC 2016), Busan, Korea* (JACoW, Geneva, 2016), <http://jacow.org/ipac2016/papers/thpor047.pdf>.